Potential of e-Fischer Tropsch Diesel and Oxymethyl-ether (OMEx) as fuels for the dual-mode dual-fuel concept

Antonio García[a,*], Javier Monsalve-Serrano[a], David Villalta[a], Rafael Lago Sari[a], Victor Gordillo Zavaleta[b], Patrick Gaillard[b]

[a]CMT - Motores Térmicos, Universitat Politècnica de València, Camino de Vera s/n, 46022 Valencia, Spain
[b]Aramco Fuel Research Center, Paris, France

Applied Energy, Volume 253, 1 Nov 2019, 113622

https://doi.org/10.1016/j.apenergy.2019.113622

Corresponding author (*):
Dr. Antonio García (angarma8@mot.upv.es)
Phone: +34 963876574
Fax: +34 963876574

Abstract

The dual-mode dual-fuel combustion strategy allows operating over the entire engine map by implementing a diffusive dual-fuel combustion at high engine loads. This requires increasing the amount of exhaust gas recirculation to control the NOx emissions, which penalizes the soot levels. At these conditions, the use of non-sooting fuels as the e-Fischer Tropsch Diesel (e-FT) and oxymethylene dimethyl ethers (OMEx) could be a potential way to avoid the NOx-soot trade-off. The experimental results acquired in a compression ignition multi-cylinder medium-duty engine evidence that the higher oxygen content of OMEx allows reducing the soot emissions at high loads to near zero levels, while e-FT promotes a soot reduction of around 20% as compared to diesel. Nonetheless, the low lower heating value of OMEx leads to excessive injection durations, enlarging the combustion process and increasing the fuel consumption around 1.3-7.2% and 1.4-5.3% as compared to diesel and e-FT, respectively, depending on the engine load. Finally, the well to wheel analysis confirms the potential in reducing the carbon dioxide footprint of OMEx (14.8-69%) and e-FT (0.3-38.5%) compared to diesel, as they can be synthetized via direct air capture as a source of carbon and using renewable energy.

Keywords

Dual-fuel combustion; emissions; soot reduction; oxygenated fuels; synthetic fuels

1. Introduction

The recent discussions about the energy source that will power the next generation vehicles have not yet reached a singular solution. In this sense, current studies show that the vehicle platform and the geographic zones in which they are used are determinant variables on the energy issue equation [1]. Nonetheless, several works still point the internal combustion engines (ICE) to remain as the major propulsive system for the next years [2]. This fact evidences the necessity of continuing with the fuels and powertrains development [3].

The future fuels must be scalable, extractable from different sources, and present good combustion properties [4]. On the other hand, the combustion devices must be able to extract as much work as possible from the fuel while minimizing the final emissions at affordable cost [5]. Despite the heavy-duty vehicles represent a small portion of the global vehicle fleet, they emit almost half of the total CO_2 emissions from the road transport, which justifies the continuous evolution of the emissions policies during the last years [6]. The proper design of both fuel and combustion devices will contribute to meet the current and future emissions regulations, with special attention to the carbon dioxide (CO_2) emissions, which must be reduced by 15% over the next few years for heavy-duty vehicles [7]. This is a challenging scenario for the ICEs since the previous statements mean, *a priori*, a direct reduction in the fuel consumption while reducing the engine-out emissions at the same time [8].

This global context has pushed the development in the powertrain field during the last few years [9]. Examples of the different strategies developed during the last years are the gasoline direct injection engines [10], downsizing techniques, higher injection pressure in diesel engines, after-treatment developments [11], understanding of the heat transfer mechanisms [12], energy losses sources in the combustion [13][14], and better materials allowing for increased mechanical constraint values, among others. However, these strategies are not enough to achieve the future requirements in terms of engine-out emissions and efficiency. To try to reach this goal, advanced combustion techniques are being develop [15]. Among the different concepts, the low temperature combustion (LTC) modes are one of the most successful strategies [16]. In general, the use of highly diluted charges [17] with premixed fuel leads to ultra-low NOx and soot emissions while presenting high fuel conversion efficiency values [18]. Nonetheless, these concepts are restricted to narrow zones inside the engine map due to the appearance of high pressure gradients at high load [19] and combustion instability with high carbon monoxide (CO) and unburned hydrocarbon emissions (HC) at low load [20].

Recently, the understanding of the fuel oxidation kinetics and the effect of the initial conditions on the combustion process allowed the development of the reactivity controlled compression ignition (RCCI) combustion strategy [21][22]. This LTC mode is based on using two fuels with different reactivity to promote a reactivity stratification inside the cylinder [23][24]. Therefore, the reaction rate can be tailored by modifying the equivalence ratio and fuel octane number stratification inside the combustion chamber, which allows a greater control of the combustion process while maintaining low emissions levels [25][26]. Nonetheless, the RCCI mode is limited to medium load conditions [27][28], being not able to cover all the engine map [29][30]. To avoid this issue, Benajes et al. [31] developed a dual-mode dual-fuel (DMDF) combustion concept switching from RCCI to a partially premixed combustion at conditions where the use of a fully premixed combustion as RCCI is limited. With this approach, the dual-fuel combustion operation can be extended to the whole engine map by promoting a more diffusive combustion at high loads. This strategy increases the soot generation at high load, and therefore high exhaust gas recirculation (EGR) levels cannot be used to reduce the NOx formation [32]. Thus, to try to reduce both emissions simultaneously, it is necessary to modify the hardware and/or of the fuel properties. Among them, the second approach has greater potential because it does not entail modifications of the

current hardware and the properties of the fuels (as per example be renewable) can add extra gains from a global point of view [33].

The literature shows important advances in fuel development, by which it is possible to obtain fuels that are able to improve the combustion process with a reduction of CO_2 emissions during their life cycle [34][35]. Among them, e-Fischer-Tropsch diesel (e-FT) is a potential fuel to be used in diesel engines with characteristics that enable soot formation reduction during its combustion. e-FT is obtained by processing syngas, a mix of CO and H_2, at temperatures in the range of 150 to 300°C and pressures ranging from one to several tens of atmospheres. The fuel obtained is highly paraffinic, with similar qualities of that of hydrogenated vegetable oils (HVO). CO and H_2 can be traditionally co-produced from hydrocarbon-based feedstock using processes like gasification or steam reforming, but they can also be produced independently and mixed in the right proportions. Hydrogen can be produced by water electrolysis using renewable electricity, and CO can be obtained by reverse water-gas shift (RWGS) of CO_2 captured from ambient air, also using a renewable source to provide thermal energy. The fact that hydrogen is produced from a non-hydrocarbon source and that CO_2 is extracted from direct air capture (DAC), and that both processes can consume renewable energy can provide CO_2 savings. A main advantage of the e-FT is its simple composition, without the presence of poly aromatic hydrocarbons and sulfur, thus favoring the reduction of the soot formation during the combustion process. Finally, the absence of aromatics together with the high paraffinic content results in a high cetane number for this fuel.

Oxymethylene dimethyl ethers (OMEx) are promising e-fuels as they allow for drastic reduction of soot formation [36]. Their production process involves several conversion steps being commonly obtained from methanol as an intermediate [37][38]. This one can be directly produced by the reaction of H_2 and CO_2, which justifies the e-fuel potential of OMEx [39]. The average efficiency of the production process of OME_{3-5} from H_2 is comparable to the efficiencies obtained in the Fischer-Tropsch (FT) diesel or methanol-to-gasoline concepts [40]. Nonetheless, if the electrical energy demand is taken into account, as well as the electrolysis efficiency, OMEx still ranks lower than others e-fuels as dimethyl ether (DME) and methanol [41]. Additionally, OMEx has a low value of lower heating value (LHV), increasing its volumetric fuel consumption. The low LHV results from the low carbon and hydrogen content in the blend, since almost half of the molecule is composed by oxygen. In some cases, they are mixed with high-energy content fuels as diesel or e-FT in different percentages to overcome this issue [42].

Investigations addressing the use of these fuels in advanced combustion concepts are still scarce. In the case of the application of the OMEx in DMDF combustion concept, there are no published works in the literature. Therefore, the present work aims to assess the combustion process and emissions characteristics of the DMDF combustion concept operating with pure e-FT and OMEx as high reactivity fuels at different engine loads. This enables exploration of the potential for reducing soot to obtain normative values in the entire engine map. The results with e-FT and OMEx are compared to diesel-gasoline operation at the same conditions. A well to wheel analysis is performed to determine the reduction potential of the CO_2 footprint taking into account the complete fuel cycle.

2. Materials and methods

2.1. Engine characteristics

A multi-cylinder, production 8L engine was used to develop the experimental investigation. Previous studies were performed on this engine platform to optimize the piston bowl geometry for the current combustion mode [24]. Different geometric modifications and auxiliary devices were added to enable the DMDF operation. The original compression ratio of this engine was reduced from 17.5:1 to 12.75:1 to decrease the mechanical demand at high loads. Additionally, a low-pressure exhaust gas recirculation system was installed with the aim of providing an additional EGR route without reducing the mass flow at the turbine inlet. This solution provides flexibility on the turbine with the possibility to achieve high total EGR rates. This solution provides the ability to regulate the EGR temperature close to the air inlet by means of a cooling circuit. Table 1 summarizes the main characteristics of the engine.

Table 1. Engine characteristics.

Engine Type	4 stroke, 4 valves, direct injection
Number of cylinders [-]	6
Displaced volume [m^3]	0.0077
Stroke [m]	0.135
Bore [m]	0.110
Piston bowl geometry [-]	Bathtub
Compression ratio [-]	12.75:1
Rated power [kW]	235 @ 2100 rpm
Rated torque [Nm]	1200 @ 1050-1600 rpm

2.2. Test cell description

Figure 1 presents the experimental facility used to perform the engine tests. The test cell is composed of three major groups: control systems, measurement devices and acquisition systems. The first group comprehends the devices that are used to control the injection systems as well as the engine speed and load. The low reactivity and high reactivity fuel injection systems are controlled by a NI PXIe 1071 board with an in-house interface built in LabView. The injection signals are crank angle referenced by an encoder, allowing to define their start and duration. The same board is used to control external devices as the back-pressure valve and the low pressure EGR quantity. Regarding the engine load and speed, both are controlled by an active dynamometer from AVL that provides a user-friendly interface, AVL PUMA open.

The second group addresses the measurement devices responsible to obtain the different quantities of interest. Engine-out gaseous emissions were measured by means of a five-gas Horiba MEXA-7100 DEGR analyzer. Smoke emissions were measured in filter smoke number (FSN) units using an AVL 415S smoke meter. For each operating condition, three consecutive measurements of 1-liter volume each with paper-saving mode off were took [43]. Two AVL 733 S balances were used to obtain the instantaneous fuel consumption of the high and low reactivity fuels while air mass flow was obtained by an Elster RVG G100 sensor. Average temperature and pressure signals were monitored at several important locations, as presented in Figure 1. In-cylinder pressure signals from the six cylinders were recorded by Kistler 6125C pressure sensors and the

crank angle was related by an AVL 364 encoder with a resolution of 0.2 crank angle degree (CAD). These signals were acquired by means of the same NI PXIe 1071 board previously mentioned. A real-time processing routine developed in Labview was used to obtain combustion information from the instantaneous aforementioned signals. Finally, the average signals were recorded by the AVL Puma interface at an acquisition rate of 10 Hz. Table 2 presents the accuracy of the main elements of the test cell.

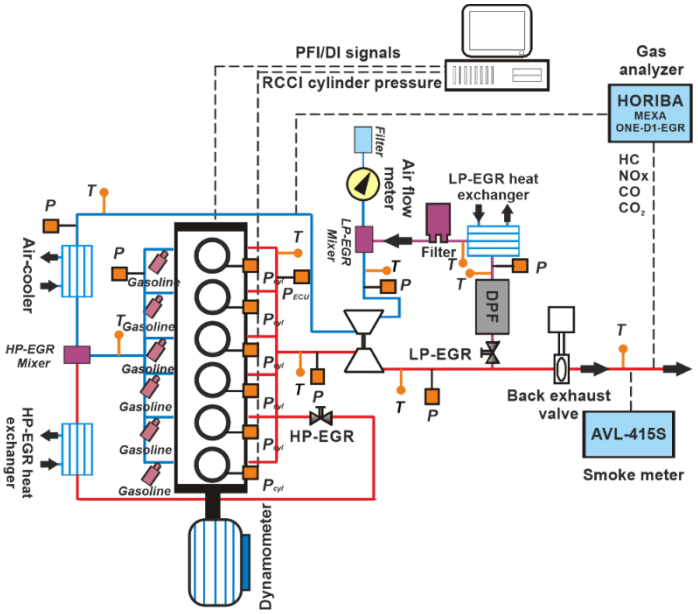

Figure 1. Experimental facility scheme.

Table 2. Accuracy of the instrumentation used in this work.

Variable measured	Device	Manufacturer / model	Accuracy
In-cylinder pressure	Piezoelectric transducer	Kistler / 6125C	±1.25 bar
Intake/exhaust pressure	Piezoresistive transducers	Kistler / 4045A	±25 mbar
Temperature in settling chambers and manifolds	Thermocouple	TC direct / type K	±2.5 °C
Crank angle, engine speed	Encoder	AVL / 364	±0.02 CAD
NOx, CO, HC, O_2, CO_2	Gas analyzer	HORIBA / MEXA 7100 DEGR	4%
FSN	Smoke meter	AVL / 415	±0.025 FSN
Gasoline/diesel fuel mass flow	Fuel balances	AVL / 733S	±0.2%
Air mass flow	Air flow meter	Elster / RVG G100	±0.1%

2.3. Fuels and injection systems characteristics

Table 3 presents the main characteristics of the high reactivity fuels (HRFs) evaluated (diesel, e-FT and OMEx). Characteristics of the commercial gasoline used as a low reactivity fuel (LRF) for all the HRFs are also shown in Table 3.

Table 3. Physical and chemical properties of gasoline and the different high reactivity fuels evaluated.

	EN 228 gasoline	EN 590 diesel	e-FT	OMEx
Density [kg/m^3] (T= 15 °C)	720	842	832	1067
Viscosity [mm^2/s] (T= 40 °C)	0.545	2.929	3.25	1.18
Cetane number [-]	-	55.7	75.5	72.9
Carbon content [% m/m]	-	86.2	85.7	43.6
Hydrogen content [% m/m]	-	13.8	14.3	8.82
Oxygen content [% m/m]	-	0	0	47.1
RON [-]	95.6	-	-	-
MON [-]	85.7	-	-	-
Lower heating value [MJ/kg]	42.4	42.44	44.2	19.04

Table 4 summarizes the characteristics of the injection systems used to provide the necessary LRF and HRF during the engine operation. The HRFs were injected into the cylinder using the stock common-rail fuel direct injection (DI) system, with a centrally located seven-hole solenoid injector. The injection pressures for the HRF ranged from 600 to 2000 bar according to the operating condition. For all the tests, gasoline was used as LRF and was port-fuel injected (PFI) by means of six PFIs located at the intake manifold.

Table 4. Characteristics of the direct and port fuel injectors.

Direct injector		Port fuel injector	
Actuation Type [-]	Solenoid	Injector Style [-]	Saturated
Steady flow rate @ 100 bar [cm^3/min]	1300	Steady flow rate @ 3 bar [cm^3/min]	980
Included spray angle [°]	150	Included Spray Angle [°]	30
Number of holes [-]	7	Injection Strategy [-]	single
Hole diameter [µm]	177	Start of Injection [CAD ATDC]	340
Maximum injection pressure [MPa]	250	Maximum injection pressure [MPa]	0.55

2.4. Testing methodology

Four engine loads were evaluated to obtain an overview of the general performance of each fuel at the characteristic zones of the map: fully premixed combustion (25% and 50% of engine load), partially premixed (80% of engine load) and diffusive combustion (100% load). Three of the four operating conditions were selected of medium/high load because these conditions are prone to produce more soot due to the high amount of diffusive combustion used to achieve the desired load. At these conditions, the differences among the fuels must be more evident. The original settings from the diesel-gasoline DMDF calibration were used as a start point for the different fuels except in some conditions limited by the injection settings. Later, the operating condition was refined following the methodology presented in [31], aiming to obtain the best values in terms of fuel consumption, soot and NOx emissions simultaneously.

2.5. Well to wheel analysis

The well to wheel analysis (WTW) is a tool that allows to quantify the greenhouse gases emitted during the path of a determined fuel. According to [44], this method differs from life-cycle analysis (LCA) since it does not take into account all the environmental impacts of an industrial process as the consumption of all materials

needed for the production process, minor emissions, etc. In this work, an enhanced well to wheel assessment has been performed to provide insight into the impact of using the e-fuels in the final CO_2 production. This enhanced approach takes into account the manufacturing process of the fuel but also the construction, use and end-of-life of the infrastructure required to produce it, as it is done in an LCA study. The approach does not include the life cycle of the engine and the vehicle.

The analysis carried out was divided into three different steps: well to tank (WTT), tank to wheel (TTW) and well to wheel. The functional units used for both steps corresponded to units of fuel produced expressed on an energy basis (MJ). CO_2 production, also called CO_2P, will therefore be expressed in gCO_2/MJ of fuel.

2.5.1. Well to tank analysis

This analysis comprehends the determination of the total emissions during the production, manufacture and distribution of a determined fuel and, for the synthetic fuels OMEx and e-FT, the emissions generated by the construction, use and end-of-life of the fuel production infrastructure, evenly distributed throughout the expected lifetime of such production units. The calculation of the CO_2 emissions per MJ of fuel was performed using an in-house LCA model built on the software application GaBi®, licensed by thinkstep®. CO_2P data of electricity production was obtained from databases licensed by thinkstep® [45]. The values of the total emissions produced during the manufacture and transportation of the fuel are dependent on the raw material, the conversion process chosen, and several parameters related to the production chain of the fuel; like the type of water electrolysis, the electricity mix or the thermal energy source used. Table 5 lists the values of such parameters.

The calculation was performed following an attributional approach, meaning that the values reported represent the average level of emissions expected for 1 MJ of fuel produced/burned. For processes with by-products (Fischer-Tropsch), CO_2 was allocated using the mass of the by-products as basis for distributing the emissions.

Table 5. Main life-cycle analysis model parameters assumed for the production of OMEx and FT diesel.

Parameter	Value
CO_2 source for FT and methanol production	Direct air capture
H_2 source for FT and methanol production	Alkaline water electrolysis
Thermal energy source for all processes	Electricity
Electricity source for all processes	100% Wind power or 100% PV power
Methanol production process (for OMEx)	Direct production
Allocation basis for FT process products	Mass-based attributional allocation

2.5.2. Tank to wheel analysis

The TTW analysis is based on the quantification of the total CO_2 emitted by MJ of fuel during the conversion of the chemical energy from the fuel into mechanical work by means of the combustion process. Since two different fuels are mixed during the dual-fuel combustion (LRF and HRF) and some of them are renewable, some statements and assumptions should be made:

1. OMEx and e-FT raw materials are renewable. Therefore, all the CO_2 produced during their combustion was absorbed by the direct air capture system. With this assumption, the TTW CO_2 emissions for OMEx and e-FT are considered zero.
2. From the first assumption, it is inferred that the total CO_2 emissions of the DMDF combustion mode when operating with e-FT or OMEx as HRF are a consequence of the gasoline consumed during the combustion process, which can be calculated as:

$$TTW\ CO_2\ [g/MJ] = \frac{BSCO_{2\_LRF}[g/kWh] \cdot Pb[Kw]}{\dot{m}_{HRF}\ [g/h] \cdot LHV_{\ HRF}\ [MJ/g] + \dot{m}_{LRF}[g/h] \cdot LHV_{LRF}[MJ/g]} \quad (1)$$

Where $\dot{m}$ stands for the mass flow consumption of the fuel (LRF or HRF according to the subscripts), LHV is the lower heating value of the correspondent fuel and Pb is the brake power of the operating condition. The $BSCO_{2\_LRF}$ value is obtained considering the gasoline fraction (GF) obtained from Equation 2 and the stoichiometry of the combustion process regarding the CO_2 formation for surrogate fuels defined in Equation 3. For diesel and e-FT, dodecane was used as surrogate fuel while for gasoline the surrogate used was isooctane. OMEx was considered to be composed of OME_1.

$$GF\ [\%] = \frac{\dot{m}_{gasoline}\ [g/s]}{\dot{m}_{gasoline}[g/s] + \dot{m}_{HRF}[g/s]} \quad (2)$$

For a given hydrocarbon molecule $C_xH_yO_z$, the production ratio considering the assumptions previously discussed can be defined as:

$$CO_2/fuel\ [-] = \frac{x \cdot M_{CO_2}\ [g/mol]}{M_{fuel}\ [g/mol]} \quad (3)$$

Where, M stands for the molar mass of the molecule and x is the number of carbon moles present in the fuel. Once this is obtained, the contribution of each fuel is calculated by Equation 4, where LRF_{WF} stands for the weight factor of the fuel. The same equation can be applied to obtain the weight of the HRF on the CO_2 production.

$$LRF_{WF}[-] = GF \cdot \left(\frac{CO_2/fuel_{LRF}}{CO_2/fuel_{HRF} + CO_2/fuel_{LRF}}\right) \quad (4)$$

Finally, the quantity of CO_2 produced by each fuel can be determined as:

$$BSCO_{2\_LRF}[g/kWh] = \frac{LRF_{WF}}{(LRF_{WF} + HRF_{WF})} \cdot \left(BSCO_{2\_TOTAL}\right) \quad (5)$$

In the case of diesel-gasoline combustion, used as reference for comparison, the TTW is obtained by:

$$TTW\ CO_2 = \frac{BSCO_{2\_TOTAL} \cdot Pb}{\dot{m}_{HRF} \cdot LHV_{\ HRF} + \dot{m}_{LRF} \cdot LHV_{LRF}} \quad (6)$$

3. Results and discussion

The results section is divided into three different parts. First, the combustion process with the different HRF is studied by means of the heat release analysis. After that, the performance and engine-out emissions are presented and discussed. Finally, the well to wheel analysis is presented to discuss the CO_2 reduction potential for the different fuels.

3.1. Effect of the high reactivity fuel characteristics on combustion parameters

The combustion analysis is performed for each operating point studied (25%, 50%, 80% and 100% engine load at 1800 rpm). Therefore, the effects of the different transport and combustion properties of the different fuels should be better differentiated in the heat release profiles and the characteristic times (CA50 and CA90-CA10).

Figure 2 presents the results obtained for the first condition evaluated (25%@1800 rpm). It is important to bear in mind that the results compared represent the best operating condition achieved for each fuel, which was obtained using different engine settings. As shown in Figure 2, the use of e-FT and OMEx results in an earlier combustion process as they have a greater cetane number than the commercial diesel. For these conditions, the EGR amounts used were 38%, 42% and 42.5% for diesel, e-FT and OME, respectively. It can be confirmed that higher EGR amounts are required to shift the combustion process toward positive CA50 values as the high cetane number improves the mixture reactivity. It is interesting to note that the CA50 values are scaled according to the mixture cetane number indicating the high influence of this property at this engine load. Nonetheless, the combustion duration values are weakly affected by the fuel composition, where the results are similar for the three fuels evaluated.

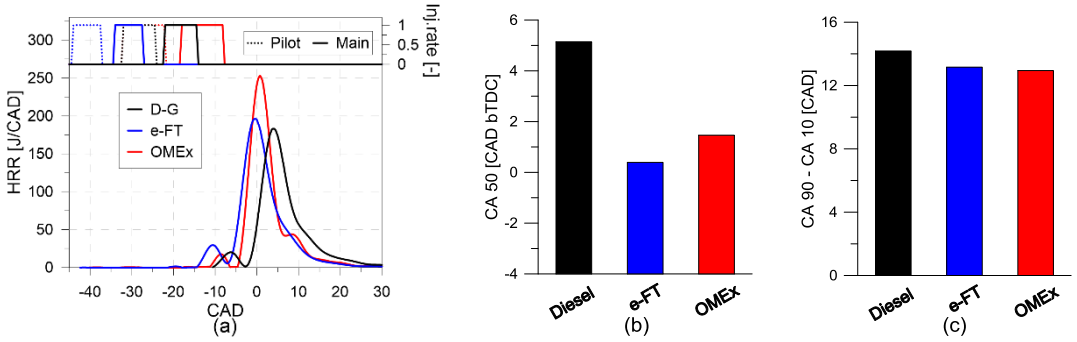

Figure 2. (a) Heat release profiles and injection rate for the pilot and main injection, (b) combustion phasing and (c) combustion duration for diesel, e-FT and OMEx for 25% of engine load and 1800 rpm.

At 50% of engine load, the differences among the combustion processes are smaller than at 25% load. This behavior can be mainly attributed to the high GF used at this

operating condition, which exceeds 70% in all the cases. By this reason, the influence of the high reactivity fuel properties is reduced. The early combustion process observed with diesel-gasoline is consequence of using an early injection timing for the HRF. This was necessary to increase the premixed fuel amount to reduce the soot formation. Nonetheless, for both e-FT and OMEx, the soot formation was not a problem during the operating condition calibration and a best phasing could be achieved. This effect was more preeminent for OMEx, where CA50 values of +4 CAD ATDC could be achieved without problems regarding engine-out soot. It is worth to state that the injection well between the pilot and main injection could not be maintained for the OMEx as a consequence of the higher energizing times required due to the lower LHV. Therefore, the pilot injection was advanced to avoid the injection overlapping promoting a higher fuel premixing, resulting in a faster combustion process as presented in Figure 3c.

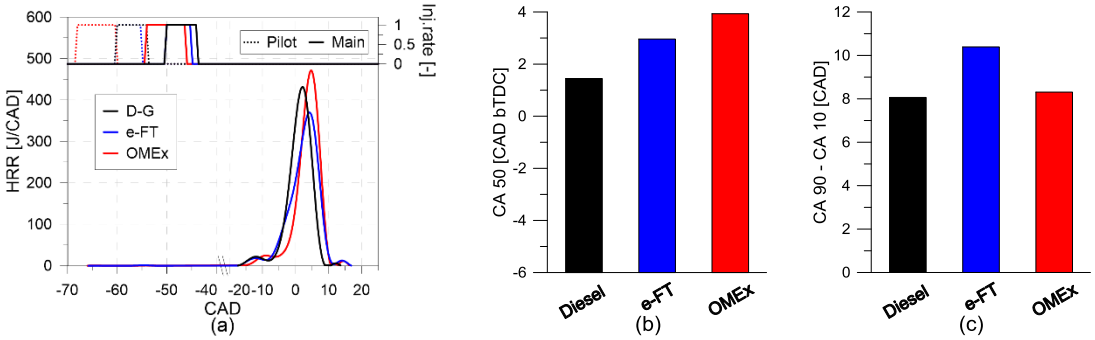

Figure 3. (a) Heat release profiles and injection rate for the pilot and main injection, (b) combustion phasing and (c) combustion duration for diesel, e-FT and OMEx for 50% of engine load and 1800 rpm.

As the engine load is increased toward the full load operation, the conditions of temperature and pressure overcome the ones required for the auto ignition of the LRF. At 80% engine load, the start of combustion is governed by the gasoline kinetics while the engine load is controlled by the amount of HRF. This can be observed in Figure 4 where the start of combustion is nearly constant for all the fuels. The combustion duration for the e-FT is slightly larger due to the slightly early start combustion. This is far inferior than the effects verified in the previous operating conditions. Another important conclusion that can be drawn from the figure analysis is the similarity between the e-FT and diesel combustion. By contrast, OMEx presents higher energy amounts released after the TDC as a consequence of the higher energizing times used to compensate the lower heating value of this fuel. Finally, the figure shows that the modification of the HRF has low impact on the combustion phasing.

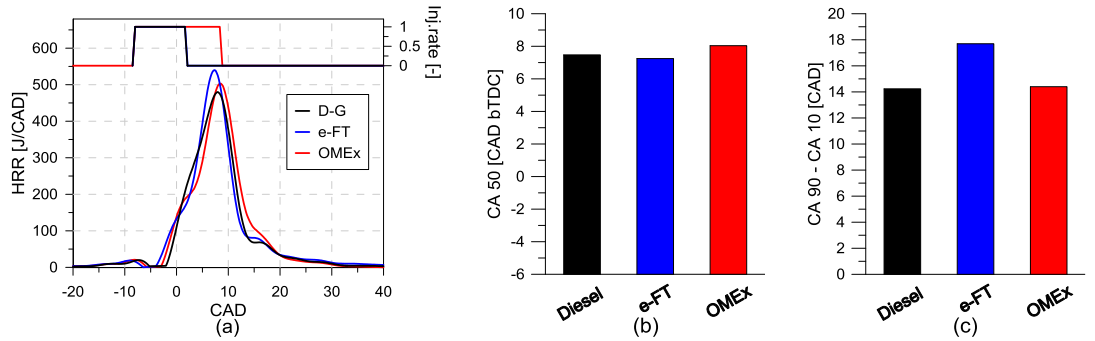

Figure 4. (a) Heat release profiles and injection rate for the pilot and main injection, (b) combustion phasing and (c) combustion duration for diesel, e-FT and OMEx for 80% of engine load and 1800 rpm.

Finally, the results at full load operation are presented in Figure 5. The major modification is observed for the OMEx combustion. In this case, the low gasoline fraction values coupled with the low LHV of this fuel requires an excessive energizing time to deliver the required HRF quantity. Therefore, the combustion process is sustained by a diffusive process during the expansion stroke, enlarging the combustion process. This fact also shifts the combustion phasing away of the firing TDC. These two effects should reduce the final efficiency of the combustion process. By contrast, the e-FT combustion is similar to that of the diesel fuel with a slightly early combustion start; which is similar to that observed in the previous operating condition.

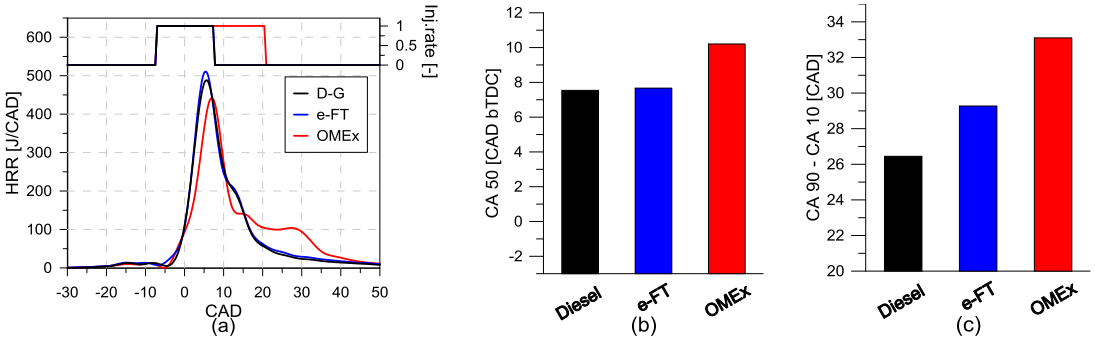

Figure 5. (a) Heat release profiles and injection rate for the pilot and main injection, (b) combustion phasing and (c) combustion duration for diesel, e-FT and OMEx for 100% of engine load and 1800 rpm.

3.2. Performance and emissions results

This section presents the performance and emissions results obtained with the different HRFs at the different operating conditions. Figure 6 illustrates the equivalent brake specific fuel consumption ($BSFC_{eq}$) as a function of the indicated mean effective pressure (IMEP). As shown in Equation 7, the equivalent BFSC takes into account the differences in LHV between the different fuels and considers the diesel fuel as a reference to maintain the same energy basis for all the mixtures. It is then possible to decouple the effects of the different LHV from the differences on the combustion process.

$$BSFC_{eq}[g/kWh] = \frac{\dot{m}_{HRF} \cdot \left(\frac{LHV_{HRF}}{LHV_{diesel}}\right) + \dot{m}_{LRF} \cdot \left(\frac{LHV_{LRF}}{LHV_{gasoline}}\right)}{P_b} \quad (7)$$

From Figure 6, different behaviors can be observed for each engine load. At ≈7 bar IMEP (25% load), e-FT presents a slightly better equivalent fuel consumption than diesel and OMEx. This is a consequence of the better combustion efficiency, since this fuel presents a higher cetane number to reduce the final amount of uHC and CO. The same impact should be verified for the OMEx. As illustrated previously in the combustion analysis, the lower LHV of this fuel requires higher injector energizing times, increasing the total combustion duration, which impairs the engine efficiency. As the load is increased to ≈12 bar IMEP (50% load), an inversion of the fuel consumption values is observed. In this case, the low LHV of the OMEx does not affect the combustion process since high levels of GF are used resulting in a high quantity of premixed fuel. Additionally, the high oxygen content in the OMEx molecule allows an increase of the EGR

concentration as much as required to obtain the normative values of soot and NOx (Figure 7) with the best combustion phasing. This is not possible for both diesel and e-FT, since they do not present oxygen in their composition being prone to produce soot.

For conditions where it is not possible to achieve a fully premixed combustion (80%/≈18 bar and 100%/≈23.5 bar of engine load), the GF must be reduced to decrease the pressure gradients. At the same time, the HRF quantity must be increased to reach the desired engine load. This action results in an issue for the OMEx application. Since its LHV is lower than half of the others, its injection duration must be enlarged by almost double to provide the same amount of energy. This has a negative impact on the combustion process, since it is enlarged toward the expansion stroke, sustained by the HRF injection. As can be seen in Figure 6, this is more evident at full load operation, where the equivalent fuel consumption values of the OMEx are considerable higher than those found for diesel and e-FT. For the last ones, their LHV allows similar fuel consumption to be obtained without impacting the final efficiency.

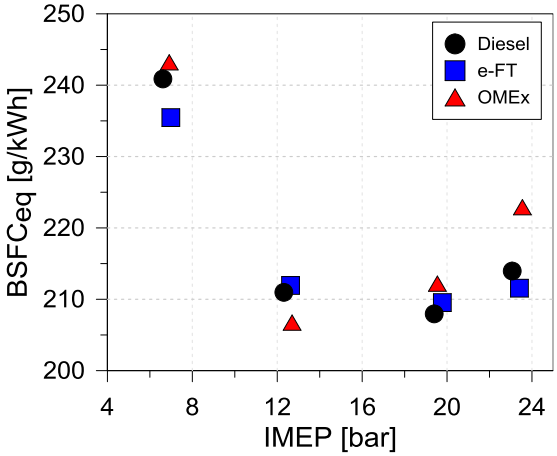

Figure 6. Equivalent brake specific fuel consumption for diesel, e-FT and OMEx at the different engine loads evaluated.

Figure 7 shows the NOx and soot emissions for the different engine loads and fuels evaluated. The NOx and soot emissions are under the EUVI normative for 25% and 50% engine load, conditions where RCCI is used. Nonetheless, as the engine load is increased, the use of diesel and e-FT does not fulfill these constraints. In these cases, the diffusive combustion results in an increase of the soot formation. Therefore, to maintain the soot values under reasonable values, the EGR rates must be decreased as changes in the injection strategy results in unacceptable values of pressure gradient and maximum pressure. As a consequence of the EGR decrease, the NOx levels also exceed the normative values. Nevertheless, the scenario is different when OMEx is used. The high oxygen content of this fuel (>40% m/m) and the molecular composition without direct bonds between carbon are factors that contribute to the soot production reduction. Therefore, the EGR concentration can be increased as much as required to reduce the NOx emissions under the normative values. The results obtained by using OMEx suggest that it is possible to obtain a calibration map with engine-out NOx and soot emissions bellow the EUVI limits. This affects directly the final cost of the after-treatment system, as devices as DPF and SCR can be removed or downsized. It should be stated that the OMEx can be blended with diesel to compensate the LHV. This will achieve the EUVI normative while maintaining injection settings closer to the diesel ones.

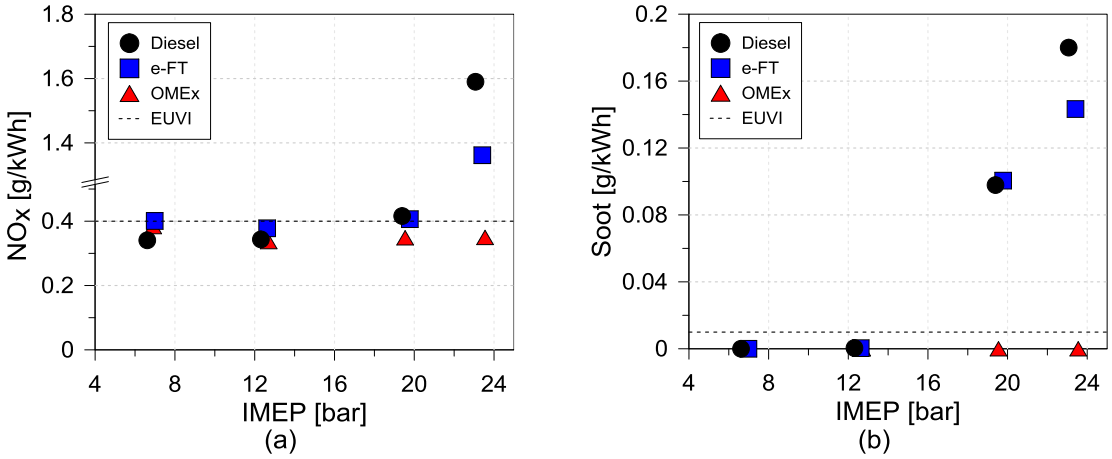

Figure 7. (a) Nitrogen oxides and (b)soot emissions for diesel, e-FT and OMEx at the different engine loads evaluated.

Finally, Figure 8 presents the unburned hydrocarbon as well as carbon monoxide emissions. The HC emissions present a monotonically decreasing trend as the engine load increases. This results from higher in-cylinder temperatures that improve the oxidation process, as addressed in the literature. In the case of DMDF combustion, this is a result of the fully premixed combustion at low engine loads, and the switch to diffusive combustion at high loads, that have characteristically low GF values and higher combustion efficiency. At 25% of engine load, where none of the conditions are limited by pressure gradient or soot emissions, the effect of the higher cetane number is apparent. As can be seen, the results are scaled according to the cetane number of each fuel. This was hypothesized in the fuel consumption results as the main reason for improvements observed with e-FT, while OMEx was penalized by the larger combustion durations. A similar behavior is verified for CO emissions at this engine load. From 50% of engine load, the specific CO emissions increase with the engine load. The longer combustion process sustained during the OMEx combustion allows an increase in the combustion efficiency, reducing the amount of CO produced.

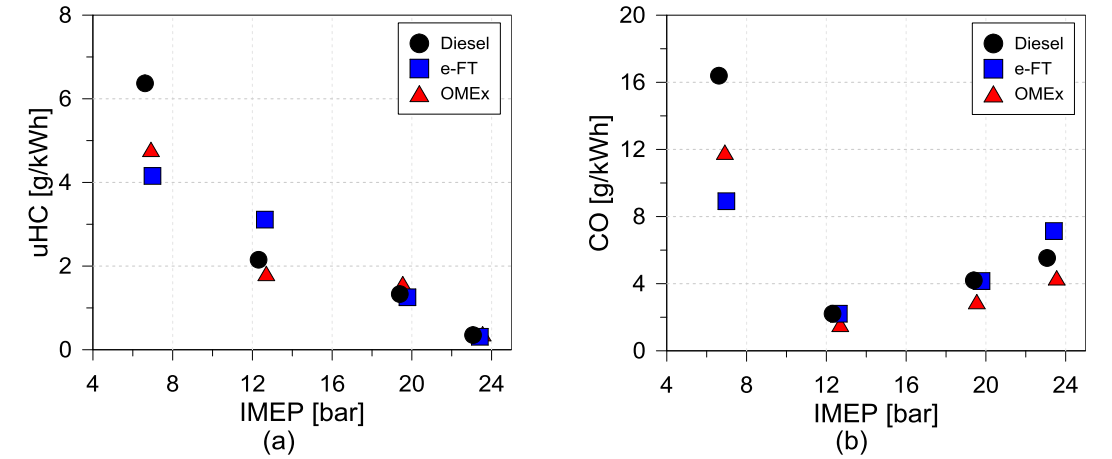

Figure 8. (a) Unburned hydrocarbon and (b) carbon monoxide emissions for diesel, e-FT and OMEx at the different engine loads evaluated.

3.3. Well to wheel assessment

3.3.1. Well to tank analysis

Figure 9 shows the results of the well to tank analysis for the different fuels as well as the different sources from which they are obtained. In the production process of OMEx, more than 80% of the input CO_2 is effectively converted into methanol to later produce the synthetic fuel. The value of CO_2 for OMEx from photovoltaic power is considerably higher than the values for e-FT, OMEx from wind power, diesel and gasoline, due to the impact of the solar panel manufacturing process. The CO_2 values of OMEx from wind power and e-FT from wind and solar power reach negative values due to the use of carbon obtained from direct air capture combined with renewable power obtained from a source of very low carbon footprint. The CO_2 values to obtain diesel and gasoline are lower than OMEx from photovoltaic power since their obtaining processes are well addressed and optimized. Differences between diesel and gasoline are related mainly to the pyrolysis and hydrotreating processes that demand higher energy in the case of diesel during its production process [45].

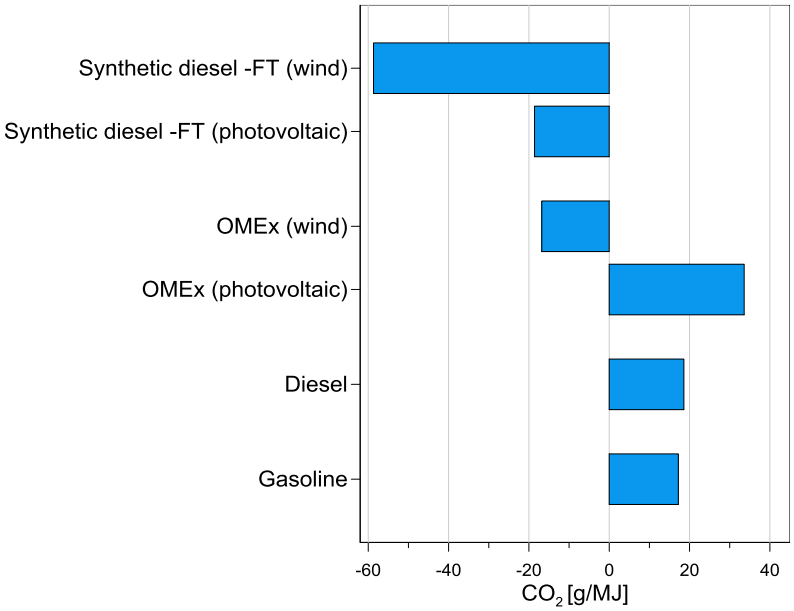

Figure 9. Well to tank CO_2 emissions for the different high reactivity fuels and gasoline considering different raw materials or different electricity sources.

3.3.2. Tank to wheel analysis

The total CO_2 produced during the combustion process of the different fuels is presented in Figure 10. The CO_2 values from the diesel-gasoline combustion are nearly constant for the different engine loads. This is a consequence of the similar amount of CO_2 produced by both fuels, which smooths the effects of the GF variation. By contrast, e-FT and OMEx are both considered renewable fuels and, consequently, the CO_2 produced by them during the combustion process is considered zero. In this sense, the final CO_2 values are only attributed to the GF used for each operating condition. As the GF values with OMEx are considerably lower due to the extra HRF quantity required to balance the low LHV of this fuel, the final CO_2 produced is also decreased. The GF values are presented in Table 6 to better illustrate this trend. In the case of e-FT, the gasoline

fractions are similar to those from diesel, and therefore the major reduction comes only from the assumption of zero CO_2 emissions by the HRF.

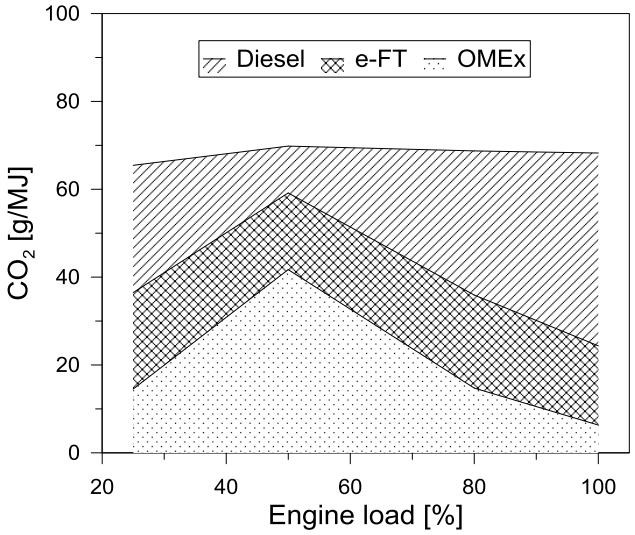

Figure 10. CO_2 tank to wheel production for diesel, e-FT and OMEx at different engine loads.

Table 6. Gasoline fraction values for each operating condition and different HRF.

	25% load	50% load	80% load	100% load
Diesel	44.08	79.93	54.71	34.22
e-FT	55.70	89.02	53.87	36.91
OME	34.53	72.07	34.26	17.25

3.3.3. Well to wheel analysis

The amount of CO_2 emitted by one fuel from its manufacturing up to its consumption in the engine (well to wheel) can be obtained by summing up the results from the WTT and TTW. Figure 11 shows the well to wheel results for the different fuels at the different loads. Among them, e-FT from wind power promotes the greatest CO_2 reduction, with negative values in almost all the operating conditions. The use OMEx also reduces the total CO_2 amount produced. Nonetheless, it is interesting to note that this trend is strongly related to the GF levels used at each operating condition.

From these results, it is clear that renewable fuels can replace the commercial diesel in a straight way to reduce the global amount of CO_2 emitted. Nonetheless, to make effective this potential, it is needed to promote changes in the legislation to consider the whole carbon cycle instead of only considering the CO_2 produced by the combustion process (TTW).

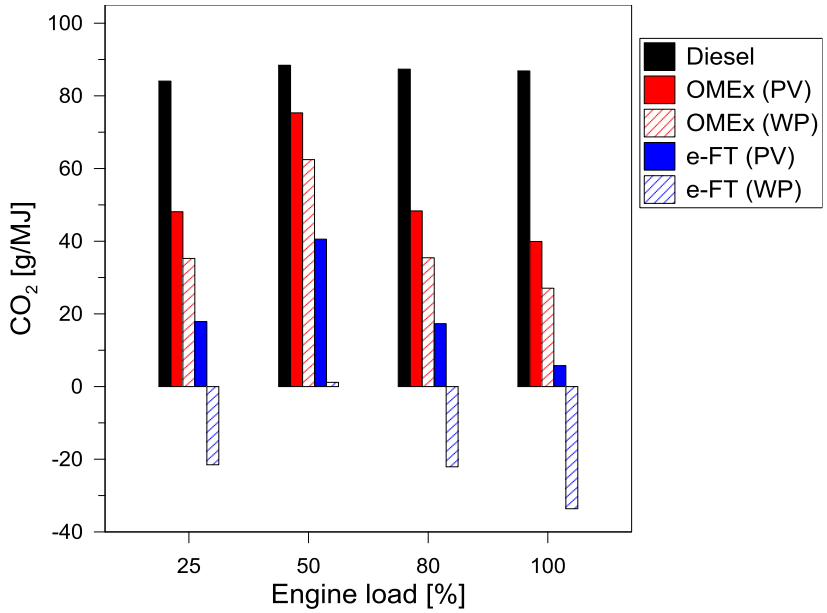

Figure 11. Well to wheel CO_2 production at different engine loads for the diesel, e-FT, photovoltaic OMEx and wind power OMEx.

4. Conclusions

This paper evaluated the combustion, performance and emissions of a multi-cylinder engine platform operating in DMDF combustion with different high reactivity fuels: diesel, OMEx and e-FT. The experimental results showed that:

- At low loads, the direct replacement of conventional diesel by e-FT improves the BSFC around 2.24%, while the use of OMEx worsens the BSFC by 1%.
- At these loads, the cetane number was found to have a major impact on the combustion development, resulting in an early combustion process for both alternative fuels.
- The use of e-FT at full load leads to soot reductions of around 0-20% as compared to diesel. These improvements are not enough to enable an effective engine recalibration to reduce the NOx (1.4 g/kWh) and BSFC (211 g/kWh).
- The use of OMEx allowed reaching zero soot levels form low to full load as a consequence of its high oxygen content and molecular structure. Thus, it was possible to increase the EGR rate to achieve EURO VI NOx values at full load at the expense of increasing the BSFC (222 g/kWh).
- The use of OMEx worsened the fuel consumption due to the higher combustion duration because of the larger energizing times associated to its low LHV. Thus, OMEx-diesel and OMEx-e-FT blends will be evaluated in future works to keep the soot potential while increasing the energy content of the final mixture.

The main conclusions from the well to wheel analysis are summarized as follows:

- The CO_2 reduction with e-FT as compared to diesel present the highest values, with WTW negative values. The OMEx presents great CO_2 benefits, with reductions compared to diesel that arrive up to 68%. This reduction with the OMEx from wind power can be attributed to the low CO_2 cost during its production and the high mass used at the same engine condition.

Acknowledgments

The authors thanks VOLVO Group Trucks Technology and Aramco Overseas Company for supporting this research. The authors also acknowledge FEDER and the Spanish Ministerio de Economía y Competitividad for partially supporting this research through the TRANCO project (TRA2017-87694-R), and the Universitat Politècnica de València for partially supporting this research through Convocatoria de ayudas a Primeros Proyectos de Investigación (PAID-06-18).

References

[1] Mackinsey. Global Energy Perspective 2019: reference case. Available at https://www.mckinsey.com/~/media/McKinsey/Industries/Oil%20and%20Gas/Our%20Insights/Global%20Energy%20Perspective%202019/McKinsey-Energy-Insights-Global-Energy-Perspective-2019_Reference-Case-Summary.ashx. Accessed 22 April 2019.

[2] U.S. Energy Information Administration (EIA). Annual Energy Outlook 2018 with projections to 2050. https://www.eia.gov/outlooks/aeo/pdf/AEO2018.pdf. [accessed 26 Oct 2018].

[3] Kalghatgi, G. Is it really the end of internal combustion engines and petroleum in transport? Applied Energy, Volume 225, May 2018, pages 965-974.

[4] Verhelst, S., Turner, J.W.G., Sileghem, L., Vancoillie, J. Methanol as a fuel for internal combustion engines. Progress in Energy and combustion science. Volume 70, October 2019, pages 43-88.

[5] Kalghatgi, G. Development of Fuel/Engine Systems-The Way Forward to Sustainable Transport. Engineering March 2019, doi: https://doi.org/10.1016/j.eng.2019.01.009

[6] Miller, J.D., Façanha, C. The state of clean transport policy - A 2014 synthesis of vehicle and fuel policy developments. The ICCT Report 2014:73.

[7] European Parliament. CO2 emission standards for heavy-duty vehicles. Available in http://www.europarl.europa.eu/RegData/etudes/BRIE/2018/628268/EPRS_BRI(2018)628268_EN.pdf, Accessed 22 April 2019.

[8] Fontaras, G., Zacharof, N-G., Ciuffo, B. Fuel consumption and CO2 emissions from passenger cars in Europe – Laboratory versus real-world emissions. Progress in Energy and Combustion Science, Volume 60, February2017, pages 97-131.

[9] Luján, J.M., Bermúdez, V., Dolz, V., Monsalve-Serrano, J. An assessment of the real-world driving gaseous emissions from a Euro 6 light-duty diesel vehicle using a portable emissions measurement system (PEMS). Atmospheric Environment, Volume 174, Feb 2018, pages 112-121.

[10] Zhao, H. Advanced Direct Injection Combustion Engine Technologies and Development. Woodhead Publishing, 2009

[11] Breakthrough: new Bosch diesel technology provides solution to NOx problem. Available at https://www.bosch-presse.de/pressportal/de/en/breakthrough-new-bosch-diesel-technology-provides-solution-to-nox-problem-155524.html. Accessed April 2019.

[12] Olmeda, P., García, A., Monsalve-Serrano, J., Sari, R. Experimental investigation on RCCI heat transfer in a light-duty diesel engine with different fuels: Comparison versus conventional diesel combustion, Applied Thermal Engineering, Volume 144, November 2018, pages 424-436.

[13] Benajes, J., Martín, J., García, A., Villalta, D., Warey, A. Swirl Ratio and Post Injection Strategies To Improve Late Cycle Diffusion Combustion in a Light-Duty Diesel Engine. Applied Thermal Engineering, Volume 123, Pages 365-376, 2017.

[14] López, J.J., Martín, J., García, A., Villalta, D., Warey, A. Implementation of Two-Color Method to Investigate Late Cycle Soot Oxidation Process in a Ci Engine Under Low Load Conditions. Applied Thermal Engineering, Volume 113, Pages 878-890, 2017.

[15] Lucchini T., Della Torre A., D'Errico G., Onorati A. Modeling advanced combustion modes in compression ignition engines with tabulated kinetics. Applied Energy, Volume 247, 2019, Pages 537-548

[16] Pachiannan T., Zhong W., Rajkumar S., He Z., Leng X., Wang Q. A literature review of fuel effects on performance and emission characteristics of low-temperature combustion strategies. Applied Energy, Volume 251,2019,113380.

[17] Saxena S., Vuilleumier D., Kozarac D., Krieck M., Dibble R., Aceves S. Optimal operating conditions for wet ethanol in a HCCI engine using exhaust gas heat recovery. Applied Energy, Volume 116, 2014, Pages 269-277.

[18] Reitz, R.D., Duraisamy, F. Review of high efficiency and clean reactivity-controlled compression ignition (RCCI) combustion in internal combustion engines. Progress in Energy and Combustion Science. Volume 46, August 2014, pages 12-71

[19] Martins, M., Fischer, I., Gusberti, F., Sari, R. et al., "HCCI of Wet Ethanol on a Dedicated Cylinder of a Diesel Engine," SAE Technical Paper 2017-01-0733, 2017, https://doi.org/10.4271/2017-01-0733.

[20] Weall, A., Szybist, J., Edwards, K., Foster, M. et al., "HCCI Load Expansion Opportunities Using a Fully Variable HVA Research Engine to Guide Development of a Production Intent Cam-Based VVA Engine: The Low Load Limit," SAE Int. J. Engines 5(3):1149-1162, 2012, https://doi.org/10.4271/2012-01-1134.

[21] Benajes, J., Molina S, García, A., Monsalve-Serrano, J. Effects of low reactivity fuel characteristics and blending ratio on low load RCCI (reactivity controlled compression ignition) performance and emissions in a heavy-duty diesel engine. Energy, Volume 90, October 2015, pages 1261-1271.

[22] Benajes, J., Molina, S., García, A., Monsalve-Serrano J. Effects of Direct injection timing and Blending Ratio on RCCI combustion with different Low Reactivity Fuels. Energy Conversion and Management, Volume 99, July 2015, pages 193-209.

[23] Pedrozo, V.B. An experimental study of ethanol-diesel dual-fuel combustion for high efficiency and clean heavy-duty engines. (Brunel University London, 2017).

[24] Benajes, J., García, A., Pastor, J.M., Monsalve-Serrano, J. Effects of piston bowl geometry on Reactivity Controlled Compression Ignition heat transfer and combustion losses at different engine loads. Energy, Volume 98, March 2016, pages 64-77.

[25] Benajes, J., García, A., Monsalve-Serrano, J., Boronat, V. Gaseous emissions and particle size distribution of dual-mode dual-fuel diesel-gasoline concept from low to full load. Applied Thermal Engineering, Volume 120, 25 Jun 2017, pages 138-149.

[26] Benajes, J, García, A, Monsalve-Serrano, J., Sari, R. L. Fuel consumption and engine-out emissions estimations of a light-duty engine running in dual-mode RCCI/CDC with different fuels and driving cycles. Energy, Volume 157, August 2018, pages 19-30.

[27] Benajes, J., García, A., Monsalve-Serrano, J., Balloul, I., Pradel, G. Evaluating the reactivity controlled compression ignition operating range limits in a high-compression ratio medium-duty diesel engine fueled with biodiesel and ethanol. International Journal of Engine Research, Volume 18 (1-2), pages 66-80, 2017.

[28] Benajes, J., García, A., Monsalve-Serrano, J., Villalta, D. Exploring the limits of the RCCI combustion concept in a light-duty diesel engine and the influence of the direct-injected fuel properties. Energy Conversion and Management, Volume 157, 2018, pages 277-287.

[29] Pedrozo, V.B. , May, I., Zhao, H., Exploring the mid-load potential of ethanol-diesel dual-fuel combustion with and without EGR, Applied Energy, Volume 193, May 2017, pages 263-275

[30] Pedrozo, V.B., May, I., Dalla Nora, M., Cairns, A., Zhao, H., Experimental analysis of ethanol dual-fuel combustion in a heavy-duty diesel engine: An optimisation at low load, Applied Energy, Volume 165, March 2016, pages 166-182

[31] Benajes, J., Pastor, J.V., García, A., Monsalve-Serrano, J. The potential of RCCI concept to meet EURO VI NOx limitation and ultra-low soot emissions in a heavy-duty engine over the whole engine map, Fuel, Volume 159, 2015, pages 952-961, ISSN 0016-2361, https://doi.org/10.1016/j.fuel.2015.07.064.

[32] Benajes J., García A., Monsalve-Serrano J., Boronat V. Dual-fuel combustion for future clean and efficient compression ignition engines, Applied Sciences, 7 (1), 2017, 36.

[33] Huang H., Wang Q., Shi C., Liu Q, Zhou C. Comparative study of effects of pilot injection and fuel properties on low temperature combustion in diesel engine under a medium EGR rate. Applied Energy, Volume 179, 2016, Pages 1194-1208.

[34] Çay, Y., Çiçek, A., Kara, F., Sağiroğlu, S. Prediction of engine performance for an alternative fuel using artificial neural network. Applied Thermal Engineering, Volume 37, 2012, Pages 217-225.

[35] Çay Y, Korkmaz I, Çiçek A, Kara F. Prediction of engine performance and exhaust emissions for gasoline and methanol using artificial neural network. Energy, Volume 50, 2013, Pages 177-186.

[36] Omari, A., Heuser, B., Pischinger, S. Potential of oxymethylenether-diesel blends for ultra-low emission engines, Fuel, Volume 209, 2017, pages 232-237, ISSN 0016-2361, https://doi.org/10.1016/j.fuel.2017.07.107.

[37] Oestreich, D., Lautenschütz, L., Arnold, U., Sauer, J. Production of oxymethylene dimethyl ether (OME)-hydrocarbon fuel blends in a one-step synthesis/extraction procedure. Fuel, Volume 214, November 2017, pages 39-44.

[38] Burre, J., Bongartz, D., Mitsos, A. Production of Oxymethylene Dimethyl Ethers from Hydrogen and Carbon Dioxide—Part I: Modeling and Analysis for OME1. Industrial & Engineering Chemistry Research, March 2019, Volume 58, pages 4881-4889, DOI: 10.1021/acs.iecr.8b05576

[39] Toyir, J., Miloua, R., Elkadri, N.E., Nawdali, M., Toufik, H., Miloua, F., Saito, M. Sustainable process for the production of methanol from CO2 and H2 using Cu/ZnO-based multicomponent catalyst, Physics Procedia, Volume 2, Issue 3, 2009, Pages 1075-1079, ISSN 1875-3892, https://doi.org/10.1016/j.phpro.2009.11.065.

[40] Burre, J., Bongartz, D., Mitsos, A. Production of Oxymethylene Dimethyl Ethers from Hydrogen and Carbon Dioxide—Part II: Modeling and Analysis for OME3–5

Industrial & Engineering Chemistry Research, March 2019, Volume 58, pages 5567-5578, DOI: 10.1021/acs.iecr.8b05577

[41] Held, M., Tönges, Y., Pélerin, D., Hartl, M., Wachtmeister, G., Burger, J. On the energetic efficiency of producing polyoxymethylene dimethyl ethers from CO2 using electrical energy. Energy and environmental Science, January 2019, pages 1019-1034.

[42] Deutz, S., Bongartz, D., Heuser, B., Kätelhön, A., Schulze, L.L., Omari, A., Walters, M., Klankermayer, J., Leitner, W., Mitsos, A., Pischinger, S., Bardow, A. Cleaner production of cleaner fuels: wind-to-wheel – environmental assessment of CO2-based oxymethylene ether as a drop-in fuel. Energy Environ. Science, November 2017, Volume 11, pages 331-343.

[43] AVL manufacturer manual. Smoke value measurement with the filter-paper method. Application notes. June 2005 AT1007E, Rev. 02. Web:<https://www.avl.com/documents/10138/885893/Application+Notes >.

[44] Edwards, R., Larivé, J-F., Rickeard, D., Weindorf, W. Well to wheels analysis of future automotive fuels and powertrains in the European context: Well-to-Tank Appendix 2 - Version 4a. Joint Research Centre of the European Commission, EUCAR, and CONCAWE 2014:1–133. doi:10.2790/95629.

[45] Hsu, D.D. Life Cycle Assessment of Gasoline and Diesel Produced via Fast Pyrolysis and Hydroprocessing. NREEL Technical report, NREL/TP-6A20-49341.

[46] Thinkstep (2019) GaBi Life Cycle Inventory Professional database. Retrieved from http://www.gabi-software.com/support/gabi/gabi-database-2019-lci-documentation/

Abbreviations

ATDC: After Top Dead Center

BSFC: Brake Specific Fuel Consumption

CAD: Crank Angle Degree

CO: Carbon Monoxide

CO_2: Carbon Dioxide

DI: Direct Injection

DMDF: Dual Mode Dual Fuel

EGR: Exhaust Gas Recirculation

FSN: Filter Smoke Number

FT: Fischer-Tropsch

GF: Gasoline Fraction

HC: Hydrocarbons

HR: Heat Release

HRF: High Reactivity Fuel

E-FT: Hydrogenated/Hydro Treated Vegetable Oil

ICE: Internal Combustion Engine

IMEP: Indicated Mean Effective Pressure

LCA: Life Cycle Analysis

LHV: Lower Heating Value

LRF: Low Reactivity Fuel

LTC: Low Temperature Combustion

MCE: Multi Cylinder Engine

NOx: Nitrogen Oxides

OMEx: Oxymethylene Dimethyl Ethers

PFI: Port Fuel Injection

PV: Photovoltaic (power)

RCCI: Reactivity Controlled Compression Ignition

TDC: Top Dead Center

TTW: Tank to Wheel

WTT: Well to Tank

WTW: Well to Wheel